

Unified sensitivity analysis of unstable or low voltages caused by load increases or contingencies

F. Capitanescu, T. Van Cutsem, *Senior Member, IEEE*

Abstract—This paper deals with the analysis of situations where load increases and/or contingencies cause transmission voltages to become unstable or unacceptably low. Simple sensitivities are proposed to determine the relative efficiency of candidate remedial actions, which are parameter changes likely to strengthen the system. To this purpose, the sensitivities of the bus voltage magnitude experiencing the largest drop are considered. In the neighborhood of a loadability limit or a critical point, it is shown that these sensitivities and those based on eigenvalue and eigenvector computation are essentially the same. However, the proposed analysis can also deal with low but stable situations. The accuracy of the proposed sensitivities is demonstrated on the models of two real systems, in which the parameters of concern are bus power injections.

Index Terms—voltage stability, voltage security analysis, sensitivity analysis, bifurcation, eigenanalysis, quasi steady-state simulation

I. INTRODUCTION

A. Voltage security assessment

VOLTAGE security has become an important aspect of power system planning, operational planning and real-time operation [1], [2], [3]. Many Transmission System Operators (TSOs) quote voltage problems as a limiting factor to the secure operation of their systems.

Over the last 15 years, significant efforts have been directed towards the development of efficient analysis and diagnosis tools for voltage stability and security analysis [4], [5].

There are roughly speaking three main categories of Voltage Security Assessment (VSA) methods [3]:

- *Contingency Analysis*: at a given operating point, the system response to credible disturbances is assessed. Within the context of long-term voltage stability (the main focus of this paper), contingencies involve basically the tripping of transmission and generation equipments.
- *Loadability Margins*: some parameters are smoothly changed until the system reaches instability or unacceptable operating conditions. The most typical parameter change is a load demand increase. Generation decrease near the load centers can be also considered. In both cases generation is increased in a remote area, which leads to power flow increases on the transmission system. Loadability margins can be computed in the current “N” configuration. However, since many voltage instability incidents were triggered by disturbances, it is of interest

to compute post-contingency loadability margins. The latter indicate how much the system can be stressed after the contingency has taken place.

- *Secure Operation Margins*: some parameters are smoothly changed in the pre-contingency configuration, until the system response to the contingency becomes unacceptable. Secure operation margins are very meaningful for real-time operation where they refer to parameters that operators either observe or control. There is also a clear distinction between pre-contingency actions/controls taken in reaction to the increased power transfer, and post-contingency controls taken in response to the disturbance.

The most widely used tool for contingency analysis is probably the *post-contingency load flow*. The divergence of the latter may reveal the loss of a long-term equilibrium and, hence, a long-term voltage instability problem. As is well-known, this static method does not take into account the system dynamics, and may diverge for numerical reasons. In addition, in case of divergence, one is left without information on where to act on the system. For dynamic studies, the benchmark method is obviously the *multi-time-scale simulation* of short- and long-term dynamics. However, such simulations remain heavy in terms of computing time, data maintenance and output processing. *Quasi steady-state simulation* is based on time-scale decomposition. This long-term simulation method consists in neglecting the short-term dynamics, replaced by their equilibrium equations. It offers better accuracy and richer interpretations than static methods, while preserving computational efficiency.

The simplest method for determining a loadability limit consists in *repeated load flows*, performed for increasing values of the system stress, until divergence is met. Avoiding the uncertainty of load flow divergence, the *continuation power flow* allows to trace the solution path passing through the loadability limit. Another straightforward technique consists in simulating the system dynamic response to a ramp increase of demand. *Optimization methods*, on the other hand, aim at directly obtaining the limit as the solution of an optimization problem whose objective is to maximize the system stress. When the base case is infeasible (i.e. in a post-contingency voltage unstable situation), the objective can be changed into minimal load curtailment.

B. Identification of remedial actions

Besides security margin computation, it is important to determine which are the best actions to restore a given level of

The authors are with the Dept. of Electrical Engineering and Computer Science (Montefiore Institute) of the University of Liège, Sart Tilman B37, B-4000 Liège, Belgium. Thierry Van Cutsem (t.vanCutsem@ulg.ac.be) is with the Belgian National Fund for Scientific Research (FNRS)

security. This question is probably more important in the open market environment where the decision to reschedule generation or curtail load must be taken by the TSO in a transparent and widely accepted manner. This paper proposes to compute sensitivities that allow to rank the candidate remedial actions according to their relative efficiency to strengthen the system.

Sensitivities computed from the Jacobian matrix of the system load flow [6] or long-term equilibrium [8] equations have been used for a long time. Within the context of VSA, sensitivities have been proposed as voltage stability indicators [7], [5], although in practice the latter are not likely to be as meaningful as load power margins. They have been proposed also to detect the crossing of a loadability limit [8]. To this purpose, the sensitivities of the total reactive power generation to the reactive loads (more precisely their sign) turn out to be a very convenient system-wide index [9], [8], [3].

A central contribution to this problem has been provided by [10], where a general formula is obtained for the sensitivity of a loadability margin to parameters. This formula involves the left eigenvector relative to the zero eigenvalue of the Jacobian matrix computed at a saddle-node bifurcation. It has been subsequently applied to various parameters in [11].

This formula was derived within the context of loadability limit computation. An extension to the analysis of post-contingency unstable scenarios was proposed in [8], with sensitivity and eigenvector computations performed along the system trajectory. This latter technique has been applied, in corrective mode, to the determination of the minimal load shedding [12] and, in preventive mode, to the improvement of secure operation margins [13].

Another early approach to the diagnosis of voltage instability relies on the modal analysis of the reduced Jacobian of reactive power with respect to voltages [14]. Information is retrieved from eigenvectors or participation factors relative to real dominant eigenvalues. This approach can suggest instability modes at normal operating points. However, owing to nonlinearities, the analysis is more reliable when performed near loadability limits or at critical points [15], i.e. at points where the Jacobian has an (almost) zero eigenvalue. The corresponding eigenvector is included in the eigenvector of the unreduced Jacobian, and the latter can be considered.

The two approaches above identify the best remedial actions from the eigenvector of an (almost) zero eigenvalue.

C. Motivation of this work

The motivation of this work is twofold.

First, dominant eigenvalue computation methods (e.g. derived from the simultaneous iteration algorithm [2], [3]) work well in most cases; however, they may experience problems when the initial estimate of the dominant eigenvalue is not accurate enough. This is especially true when the loadability limit corresponds to a “breaking point” where a generator switches under reactive power limit [16], [3] in which case the real dominant eigenvalue jumps from a negative to a large positive value [3].

Second, in practice, voltages are often requested to stay above some thresholds (corresponding for instance to under-

voltage tripping of equipments). In some cases, these minimum voltage limits can be more constraining than voltage stability limits. If so, the system response to a load increase (resp. a contingency) will be unacceptable well before the loadability limit is reached (resp. the post-contingency evolution becomes unstable). At the last acceptable operating point, voltages are low but stable and the Jacobian eigenvalues are still on the stable side; hence, the eigenvector computation does not apply.

A unified approach that encompasses the low voltage, the zero eigenvalue and the breaking point situations is thus of interest [18]. To this purpose, we propose to replace the eigenvector computation by a simple sensitivity calculation which provides very close results, but is non iterative and can still be computed when the system reaches low but stable voltages.

This sensitivity computation is intended to be coupled with continuation power flows or time simulation (multi time-scale or quasi steady-state). It can also be used at the last converged solution of repeated load flows. In principle, it is not intended to be used with optimization methods, insofar as the dual variables (LaGrange multipliers) relative to the load flow equality constraints provide the sought eigenvector.

The paper is organized as follows. Section II derives the proposed sensitivities, compares them to the eigenvector-based approach and discusses several implementation aspects as well as extensions. Various simulation results are given in Section III. Comments on the use of the sensitivities and conclusions are offered in Sections IV and V, respectively.

D. Notation

Arrays are shown with bold letters. All vectors are column vectors.

II. PROPOSED SENSITIVITY METHOD

A. Principle

It is well known that long-term voltage instability develops as a progressive fall of transmission voltages. If snapshots are taken along an unstable system trajectory and if bus voltage magnitudes are sorted out, a most affected area can be easily pointed out. Depending upon the instability “mode”, this area may be more or less extended.

Within the context of remedial actions, it makes sense to act on the controls that will prevent the lowest transmission voltage to fall. We therefore propose:

- to consider the bus experiencing the largest voltage drop (due to the load increase when computing loadability limits, or the contingency when performing contingency analysis). We will refer to the latter as the weakest bus. Let us assume that this is the ℓ -th one;
- to identify the remedial actions able to increase the voltage magnitude V_ℓ of the weakest bus, by computing the sensitivities

$$\frac{\partial V_\ell}{\partial \mathbf{p}} = \left[\frac{\partial V_\ell}{\partial p_1} \quad \frac{\partial V_\ell}{\partial p_2} \quad \dots \quad \frac{\partial V_\ell}{\partial p_n} \right]^T \quad (1)$$

where \mathbf{p} is the vector of candidate controls. In the sequel we will mainly concentrate on bus power injections, but extension to other controls can be envisaged.

B. Sensitivity computation

We recall hereafter a general sensitivity formula [6], [17] allowing to compute (1).

Let the system be characterized by the equilibrium equations:

$$\mathbf{f}(\mathbf{x}, \mathbf{p}) = \mathbf{0} \quad (2)$$

where \mathbf{x} is the n -dimensional vector of state variables.

For a small change in \mathbf{p} , a linearization of (2) yields:

$$\mathbf{f}_x d\mathbf{x} + \mathbf{f}_p d\mathbf{p} = \mathbf{0} \quad (3)$$

where \mathbf{f}_x (respectively \mathbf{f}_p) is the Jacobian matrix of \mathbf{f} with respect to \mathbf{x} (respectively \mathbf{p}). Both matrices are sparse. Assuming that \mathbf{f}_x is nonsingular, one easily obtains:

$$d\mathbf{x} = -\mathbf{f}_x^{-1} \mathbf{f}_p d\mathbf{p} \quad (4)$$

Let $\eta(\mathbf{x})$ be a quantity of interest, function of the state variables \mathbf{x} . A small change $d\mathbf{p}$ induces a small change $d\mathbf{x}$ which in turn causes the following change in η :

$$d\eta = \sum_i \frac{\partial \eta}{\partial x_i} dx_i = d\mathbf{x}^T \frac{\partial \eta}{\partial \mathbf{x}} = -d\mathbf{p}^T \mathbf{f}_p^T (\mathbf{f}_x^{-1})^T \frac{\partial \eta}{\partial \mathbf{x}}$$

Hence, the sensitivities of η to \mathbf{p} are given by:

$$\frac{\partial \eta}{\partial \mathbf{p}} = -\mathbf{f}_p^T (\mathbf{f}_x^{-1})^T \frac{\partial \eta}{\partial \mathbf{x}} \quad (5)$$

In practice, these sensitivities are obtained by solving a linear system with \mathbf{f}_x^T as matrix of coefficients and $\partial \eta / \partial \mathbf{x}$ as right-hand side, and pre-multiplying the solution by \mathbf{f}_p^T .

In the particular case of sensitivities (1):

$$\eta = V_\ell \quad \text{and hence} \quad \frac{\partial \eta}{\partial \mathbf{x}} = \mathbf{e}_\ell \quad (6)$$

where \mathbf{e}_ℓ is the unit vector with $e_i = 0, \forall i \neq \ell$ and $e_\ell = 1$.

C. Relationship with eigenvectors

We now show that, when computed near a Saddle-Node Bifurcation (SNB) point, the sensitivities (1) provide essentially the same control ranking as the eigenvector-based formula proposed in [10], [11] and used in many publications. We also show that they can be used to compute the sensitivity of margins to parameters.

Consider the computation of a loadability limit in which the parameters \mathbf{p} are smoothly changed into $\mathbf{p} + \mu \mathbf{d}$ where \mathbf{d} is a given participation vector. The loadability margin μ^* is the maximum value of μ such that (2) still has a solution. In the absence of inequality constraints (stemming mainly from generator reactive power limits), $\mathbf{p} + \mu^* \mathbf{d}$ corresponds to an SNB point and we have:

$$\mathbf{f}(\mathbf{x}, \mathbf{p} + \mu^* \mathbf{d}) = \mathbf{0} \quad (7)$$

$$\mathbf{w}_c^T \mathbf{f}_x = \mathbf{0} \quad (8)$$

where (8) expresses that \mathbf{f}_x is singular, i.e. it has a zero eigenvalue, $\lambda_c = 0$, whose left eigenvector is \mathbf{w}_c .

The loadability margin μ^* is a measure of the system robustness at the base case operating point corresponding to $\mu = 0$. When μ^* is deemed too small, it is of interest to determine which parameters \mathbf{p} should be changed in order to

increase μ^* efficiently. It is easily shown [10], [11], [3] that the sensitivity of μ^* to \mathbf{p} is given by:

$$\frac{\partial \mu^*}{\partial \mathbf{p}} = -\frac{\mathbf{f}_p^T \mathbf{w}_c}{\mathbf{w}_c^T \mathbf{f}_p \mathbf{d}} = -\frac{\mathbf{n}}{\mathbf{n}^T \mathbf{d}} \quad (9)$$

where $\mathbf{n} = \mathbf{f}_p^T \mathbf{w}_c$ is, in the parameter space, the normal vector to the bifurcation surface characterized by (7, 8)¹.

Let us assume that \mathbf{f}_x has all distinct eigenvalues, so that its inverse can be decomposed into:

$$\mathbf{f}_x^{-1} = \sum_{i=1}^n \frac{\mathbf{v}_i \mathbf{w}_i^T}{\lambda_i} \quad (10)$$

where \mathbf{v}_i (respectively \mathbf{w}_i) is the right (respectively left) eigenvector relative to λ_i . Introducing (6, 10) into (5) yields:

$$\begin{aligned} \frac{\partial V_\ell}{\partial \mathbf{p}} &= -\sum_{i=1}^n \frac{\mathbf{f}_p^T \mathbf{w}_i \mathbf{v}_i^T \mathbf{e}_\ell}{\lambda_i} = -\sum_{i \neq c} \frac{\mathbf{f}_p^T \mathbf{w}_i \mathbf{v}_i^T \mathbf{e}_\ell}{\lambda_i} - \frac{\mathbf{f}_p^T \mathbf{w}_c \mathbf{v}_c^T \mathbf{e}_\ell}{\lambda_c} \\ &= -\sum_{i \neq c} \frac{\mathbf{f}_p^T \mathbf{w}_i \mathbf{v}_i^T \mathbf{e}_\ell}{\lambda_i} - \mathbf{n} \frac{\mathbf{v}_c^T \mathbf{e}_\ell}{\lambda_c} \end{aligned} \quad (11)$$

Now, as μ approaches μ^* , λ_c goes to zero, and the magnitude of the second term in (11) becomes larger and larger. In other words:

$$\text{for } \mu \rightarrow \mu^* : \frac{\partial V_\ell}{\partial \mathbf{p}} \rightarrow -k \mathbf{n} = k' \frac{\partial \mu^*}{\partial \mathbf{p}} \quad (12)$$

where the scalars k and k' are given respectively by:

$$k = \frac{\mathbf{v}_c^T \mathbf{e}_\ell}{\lambda_c} \quad k' = (\mathbf{n}^T \mathbf{d}) k \quad (13)$$

It results that $\partial V_\ell / \partial \mathbf{p}$, \mathbf{n} and $\partial \mu^* / \partial \mathbf{p}$ become collinear. Hence, under the above assumptions, *these three vectors basically provide the same information about the relative efficiency of the various controls.*

The equivalence can be made further explicit by rewriting (9) as follows:

$$\frac{\partial \mu^*}{\partial \mathbf{p}} = -\frac{-k \mathbf{n}}{-k \mathbf{n}^T \mathbf{d}} \simeq -\frac{\frac{\partial V_\ell}{\partial \mathbf{p}}}{\left[\frac{\partial V_\ell}{\partial \mathbf{p}} \right]^T \mathbf{d}} \quad \text{when } \mu \simeq \mu^* \quad (14)$$

which shows that, beyond ranking, the proposed sensitivities can be substituted for the eigenvector to compute the sensitivity of margins to parameters.

D. On the choice of the weakest bus ℓ

In theory, the above result holds true whatever the bus ℓ . In practice, however, the eigenvalue λ_c is close but not equal to zero. Therefore, the contribution of the first term in (11) may not be negligible. This is even more true when the system size increases, i.e. when the sum extends over a larger number of eigenvalues. In order the last term to be dominant, the value of $k = \mathbf{v}_c^T \mathbf{e}_\ell$ should be as large as possible. \mathbf{e}_ℓ being a unit

¹the sensitivity with respect to a parameter other than an injection can be obtained by adding this parameter to \mathbf{p} and assigning a zero value to the corresponding component of \mathbf{d}

vector, it is easily seen that bus ℓ should correspond to the largest entry of the right eigenvector \mathbf{v}_c .

At first glance, we are thus brought back to an eigenvector computation. Luckily, the following property, already quoted in [10], allows to avoid this computation.

Consider the variation $d\mathbf{x}$ caused by $d\mu$. Introducing $d\mathbf{p} = d\mu \mathbf{d}$ and (10) into (4) yields:

$$d\mathbf{x} = - \sum_{i=1}^n \mathbf{v}_i \frac{\mathbf{w}_i^T \mathbf{f}_p \mathbf{d}}{\lambda_i} d\mu = \left[- \sum_{i \neq c} \mathbf{v}_i \frac{\mathbf{w}_i^T \mathbf{f}_p \mathbf{d}}{\lambda_i} - \mathbf{v}_c \frac{\mathbf{n}^T \mathbf{d}}{\lambda_c} \right] d\mu \quad (15)$$

As μ approaches μ^* , the second term becomes dominant and the variation becomes

$$d\mathbf{x} \simeq k'' d\mu \mathbf{v}_c \quad \text{where } k'' = \frac{\mathbf{n}^T \mathbf{d}}{\lambda_c} \quad (16)$$

Hence, as μ approaches μ^* , the state variable experiencing the largest rate of change $|\partial x / \partial \mu|$ corresponds to the largest component of \mathbf{v}_c .

Since voltage magnitudes are the state variables likely to drop the most in voltage unstable scenarios, the weakest bus can be taken as the bus with the largest rate of decrease of the voltage magnitude.

To summarize, choosing bus ℓ as the one experiencing the largest voltage drop does not only make sense by itself but also allows the $\partial V_\ell / \partial \mathbf{p}$ sensitivities to better match the $\partial \mu^* / \partial \mathbf{p}$ sensitivities obtained from eigenvectors.

Note finally that the choice of the weakest bus is not critical inasmuch as it corresponds to a large component of \mathbf{v}_c , which reinforces the dominant character of the second term in (11).

E. Sensitivity normalization

When the aim is to display at which system buses to act, it is convenient to consider normalized sensitivities, obtained by dividing the $\partial V_\ell / \partial \mathbf{p}$ vector by its component of largest magnitude. This is especially true when the objective is to improve an insufficient loadability margin. Indeed, since the sensitivities have to be computed near the SNB where \mathbf{f}_x has an almost zero eigenvalue λ_c , the components of $\partial V_\ell / \partial \mathbf{p}$ assume very large values. In this case, the information brought by the normalized sensitivities is the relative merit and sign of the various control actions.

When the objective is to estimate the amount of control needed to restore feasibility, according to formula (14), either absolute or normalized sensitivities can be used, since this is just a matter of multiplying the $\partial V_\ell / \partial \mathbf{p}$ vector by a scaling factor, and this vector appears at both the numerator and denominator of (14).

Now, when the objective is to estimate the amount of control needed to increase a low but stable voltage, formulae (5, 6) are used. In this case, the absolute values of the sensitivities are considered.

F. Extension to contingency analysis

Within the context of contingency analysis it is of interest to identify the best remedial actions to stabilize the post-contingency evolution of the system. To this purpose, an

extension of the above computations was proposed in [8], based on a system portrait in the space of load powers. The method consists in identifying the so-called *critical point* of the system trajectory. This point is characterized by a singular Jacobian \mathbf{f}_x but is not a long-term equilibrium, i.e. it satisfies (8) but not (7). At the critical point, the normal vector \mathbf{n} to the bifurcation surface is computed and the latter is linearly approximated by its tangent hyper plane. This allows to estimate how much each injection should be varied in order to restore a long-term equilibrium to the system. It is easily shown that the injection change is inversely proportional to the component of \mathbf{n} , i.e. the larger the component, the smaller the injection change.

The method has been validated in [12] within the context of minimal load shedding and furthermore used for pre-contingency security enhancement in [13], [18].

According to (12), the sensitivities $\partial V_\ell / \partial \mathbf{p}$ computed at the critical point can be substituted for the normal vector \mathbf{n} .

G. Point of linearization

When dealing with voltage unstable situations, the above derivations have shown the necessity to compute the sensitivities $\partial V_\ell / \partial \mathbf{p}$ at the point where \mathbf{f}_x has an (almost) zero eigenvalue λ_c .

In continuation power flows, this point can be identified as corresponding to the crossing of the loadability limit, which is revealed by the decrease of load power along the solution path. In practice, the Jacobian matrices and the $\partial V_\ell / \partial \mathbf{p}$ sensitivities can thus be computed at the first point of the path where a decrease in load power is observed. In repeated load flows, the computation can be performed at the last converged point, provided that the latter is close enough to the loadability limit.

When using time simulation (for computing a loadability limit or simulating a contingency), the sign of sensitivities can be used to identify the point of the system trajectory where \mathbf{f}_x has an eigenvalue λ_c closest to zero [3], [8]. Indeed, it is easily seen from (11) that when an eigenvalue λ_c changes from a negative to a positive value, the sensitivities have larger and larger magnitudes, suddenly change sign, and then have decreasing magnitudes. The Jacobian matrices and the sensitivities can be computed at the first point where this change in sign “through infinity” occurs.

In fact, this property applies to the sensitivity of any quantity η provided that $\mathbf{v}_c^T \partial \eta / \partial \mathbf{x}$ is large enough so that the second term in (11) is dominant. For already explained reasons, this is the case for V_ℓ , the voltage magnitude experiencing the largest rate of decrease. According to our experience, this is always the case when η is chosen as the total reactive power production Q_g (of generators and compensators) and \mathbf{p} as the reactive powers of all loads. The $\partial Q_g / \partial \mathbf{p}$ sensitivities are thus also a good choice.

When crossing a breaking point, the same change in sign takes place, although the sensitivities do not go through infinity [3]. Hence, their magnitudes are significantly smaller in the neighborhood of a breaking point than around an SNB point. Nevertheless, as for an SNB, the linearization can be performed at the first point after sensitivities have changed sign, as proposed and validated in [12], [13].

III. NUMERICAL RESULTS

Quasi Steady-State (QSS) simulation has been used in the simulations reported hereafter. The Jacobian matrix \mathbf{f}_x relates to the long-term equilibrium equations as detailed in [3], [8].

A. Test systems

The results presented in this section relate to two real power systems, whose model is first outlined.

The first system is the one operated by RTE, the French Transmission System Operator (formerly EDF). Although its network is rather dense and meshed, much attention is paid to voltage security in the Western and Southeast regions where load centers are farther away from generation. The QSS model includes 1715 buses, of which 1203 are transmission buses at the EHV (400 and 225-kV) level. Voltage dependent loads are fed through two transformers in cascade. The upper ones correspond to the real EHV-HV transformers feeding the HV (90- and 63-kV) sub-transmission system, while the lower ones are equivalent accounting for HV-MV distribution transformers. The QSS simulation focuses on the long-term dynamics of 1024 Load Tap Changers, 176 overexcitation limiters and 15 secondary voltage controllers represented in the Western and Southeast regions.

The second system is operated by Hydro-Québec (HQ). It is characterized by great distances (more than 1000 km) between the large hydro generation areas of James Bay (JB), Churchill Falls (CF) and Manic-Outardes (MO), and the main load center around Montréal and Québec City (MQ). A large part of the 735-kV transmission system is located in two corridors. The system is limited by angle stability in the North and voltage stability in the South, near the MQ area. Besides static var compensators and synchronous condensers, the automatic shunt reactor switching devices play an important role in voltage control. They operate with delays upon measurement of low or high voltages. The post-contingency evolution of the system is much influenced by these controls.

In both systems, loads are represented by an exponential model

$$P = P_o(V/V_o)^\alpha \quad Q = Q_o(V/V_o)^\beta \quad (17)$$

with various values of α and β according to the nature of loads.

B. Validation of sensitivities in loadability limit computation

We first present results dealing with the determination of loadability limits on the RTE system.

To this purpose, the P_o and Q_o coefficients in (17) are smoothly increased linearly with time. For the whole system, a ramp of 10000 MW / 4000 Mvar over 1000 s is considered, compensated by French generators. A $\partial Q_g/\partial Q_\ell$ sensitivity computed along this trajectory is shown in Fig. 1. The sign change described in Section II.G is easily seen at $t = 930$ s.

The bus experiencing the largest drop is located in the Southeast region and its voltage is taken as V_ℓ (Fig. 1 refers to this bus in fact). The sparse Jacobian matrix \mathbf{f}_x and therefrom the vectors of sensitivities $\partial\mu^*/\partial\mathbf{p}$ and $\partial V_\ell/\partial\mathbf{p}$ are computed at the first point after the sign changes.

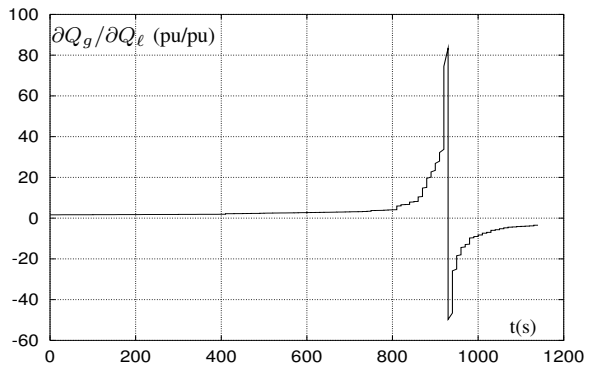


Fig. 1. Evolution of a $\partial Q_g/\partial Q_\ell$ sensitivity during load increase

Figure 2 shows the largest components relative to active and reactive power injections, respectively. Each sub-vector has been normalized so that its largest component is equal to 1 (see Section II.E). As can be seen, there is a very good agreement between the eigenvector-based sensitivities (solid lines) and the proposed simpler sensitivities (dashed lines). Both lead to very close rankings of bus injections. This result is noteworthy considering that \mathbf{f}_x is a 4470×4470 matrix and, hence, 4469 eigenvalues contribute to the first term of (11).

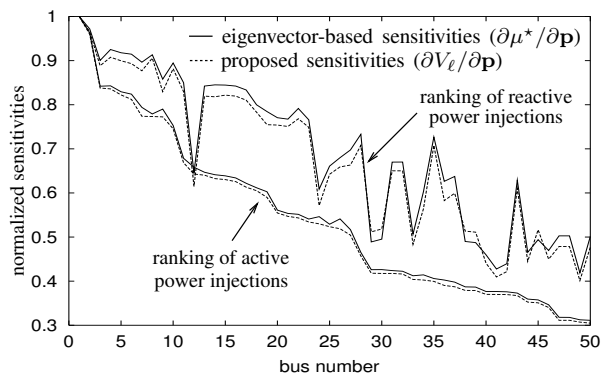


Fig. 2. RTE system : ranking of active and reactive bus power injections near SNB point

C. Validation of sensitivities in contingency analysis : RTE system

We show next the validity of the proposed sensitivities to diagnose situations where the system is unstable (or has very little security margin) following contingencies. In this case, the normal vector \mathbf{n} and the $\partial V_\ell/\partial\mathbf{p}$ sensitivities are computed at the critical point of the post-contingency system evolution (see Section II.F).

We consider a contingency whose secure operation margin is 4800 MW (of national load increase). In the shown example, the load is first increased by 4900 MW, then the contingency is applied, which causes long-term voltage instability. Sensitivities of the type shown in Fig. 1 indicate that the critical point is crossed 130 s after the contingency occurrence.

Figure 3 shows the normalized components of \mathbf{n} and $\partial V_\ell/\partial\mathbf{p}$, relative to the active powers of 19 influencing gen-

erators for this contingency. This information is of interest in congestion management when it is relevant to optimally modify the generation scheme. Here too, the two rankings are in very good agreement, with only a small discrepancy for generators 2 to 6.

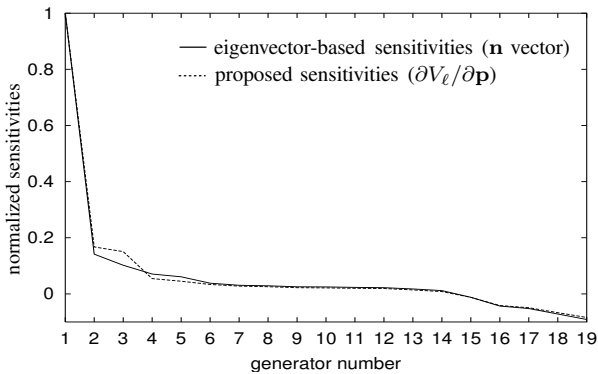


Fig. 3. RTE system : ranking of active power generations near critical point

D. Validation of sensitivities in contingency analysis : HQ system

1) *Contingency C1*: We first consider a 735-kV line tripping contingency in the JB corridor. Figure 4 shows the time evolution of the voltage which drops the most under the effect of the contingency. The system is stabilized by the tripping of several shunt inductors. However, the system is insecure since a pre-contingency load increase of only 160 MW would lead to post-contingency instability (which is below the usual thresholds used by HQ). The usual change in sign of $\partial Q_g/\partial Q_\ell$ is observed 20 s after the contingency occurrence while the reverse change is observed 143 s later, indicating that the system has come back above the critical point owing to the shunt reactor trippings. This is confirmed by the values of the dominant eigenvalue λ_c shown in Fig. 4.

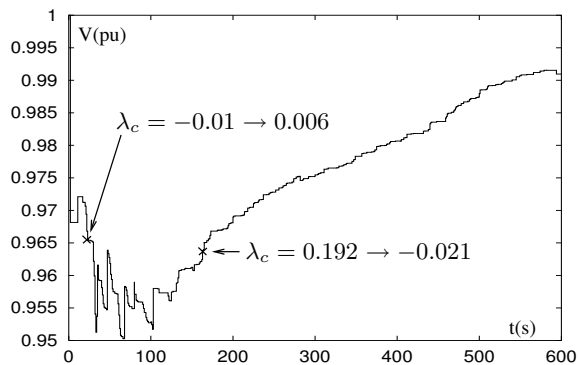


Fig. 4. Voltage at a 735-kV bus after contingency C1

The \mathbf{n} and $\partial V_\ell/\partial \mathbf{p}$ vectors are computed at the first met critical point. The corresponding ranking of 84 active power generations is shown in Fig. 5. The agreement is perfect with the two curves hardly discernible. Positive sensitivities indicate generators that should have their production increased;

expectedly, they are located either close to the MQ load area or in the CF-MO corridor not affected by the contingency.

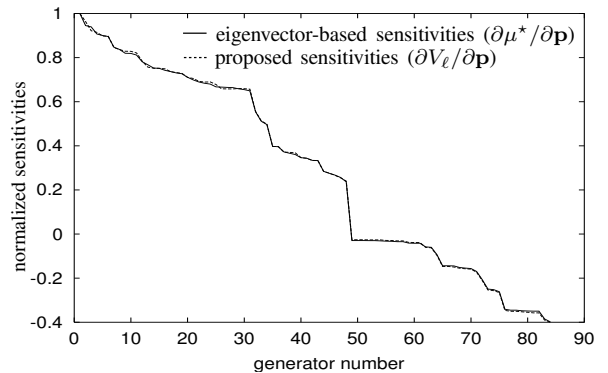


Fig. 5. HQ system: ranking of active power generations for contingency C1

2) *Contingency C2*: We next consider a 735-kV line tripping contingency in the CF-MO corridor, under stressed operating conditions, leading to the unstable voltage evolution shown in Fig. 6. This case is severe in the sense that the $\partial Q_g/\partial Q_\ell$ sensitivities change sign right after the contingency. As indicated in Fig. 6, the dominant eigenvalue does not pass smoothly through zero but rather jumps to a relatively large value (0.551 to be compared with 0.006 in Fig. 4). In the absence of a better linearization point, the sensitivity analysis is performed at this point.

The corresponding ranking is shown in Fig. 7. For some generators, the normalized components of \mathbf{n} and $\partial V_\ell/\partial \mathbf{p}$ are somewhat different. This is attributable to the fact the second term in (11) is less dominant in this example than in the previous one. However, no generator experiences a major change of its ranking.

Note finally that, in view of the assumptions underlying the use of \mathbf{n} , the $\partial V_\ell/\partial \mathbf{p}$ sensitivities appear as an equally acceptable, while more “transparent” ranking criterion.

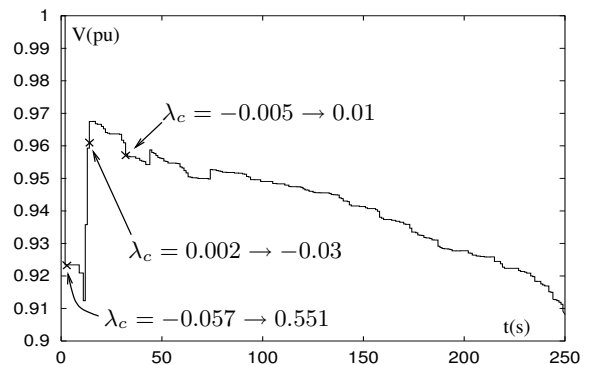


Fig. 6. Voltage at a 735-kV bus after contingency C2

E. Influence of weakest bus ℓ

It has been explained in Section II.D why it is appropriate to chose V_ℓ as the voltage magnitude with the largest rate of decrease, at least when computing a loadability limit.

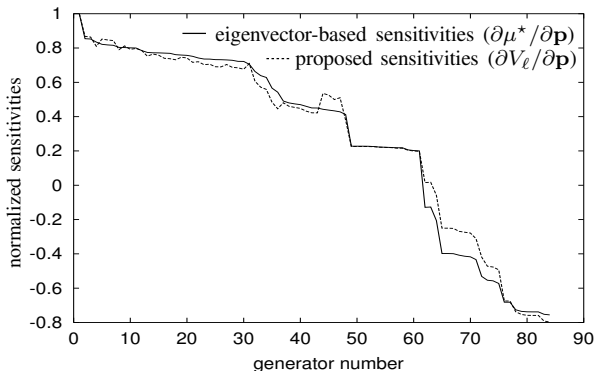


Fig. 7. HQ system: ranking of active power generations for contingency C2

Figure 8 compares the generator rankings provided by $\partial V_\ell / \partial \mathbf{p}$ for four different choices of bus ℓ . It relates to the contingency analysis example of Section III.D.1, relative to the RTE system.

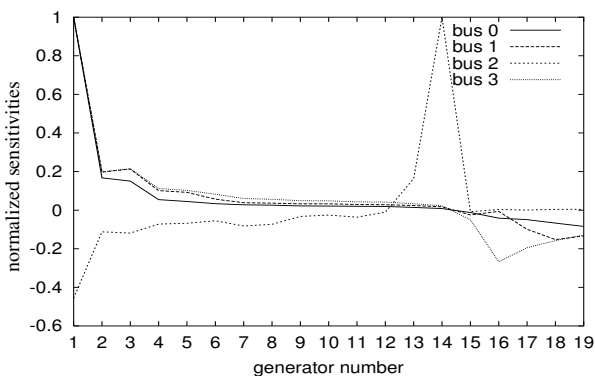


Fig. 8. $\partial V_\ell / \partial \mathbf{p}$ sensitivities for different choices of the weakest bus ℓ

Bus 0 undergoes the largest voltage drop between the pre-contingency and the critical points and is thus considered as the best choice. This bus was used for the comparison of Fig. 3, and it leads indeed to almost the same ranking as \mathbf{n} . Bus 1 is located near bus 0, in the area affected by the contingency. As can be seen, it yields almost the same ranking. Buses 2 and 3 are located at some distance, in different directions, from bus 0. The ranking of generators 16, 17 and 18 is affected when choosing bus 3, while a totally erroneous ranking is obtained when using bus 2.

These results show that the choice of bus ℓ is not critical provided that it is located in that part of the system experiencing the largest voltage drops under the effect of the contingency or the load increase.

F. Analysis of low but stable voltages

The example below illustrates the ability of the proposed sensitivities to diagnose unstable cases as well as low but stable voltage situations.

We consider the effect of a (generator tripping) contingency on the RTE system at four pre-contingency load levels. Figure 9 shows the time evolution of the transmission voltage

V_ℓ most affected by the contingency. The curves relate to different pre-contingency load increases above the base case, as indicated in the figure.

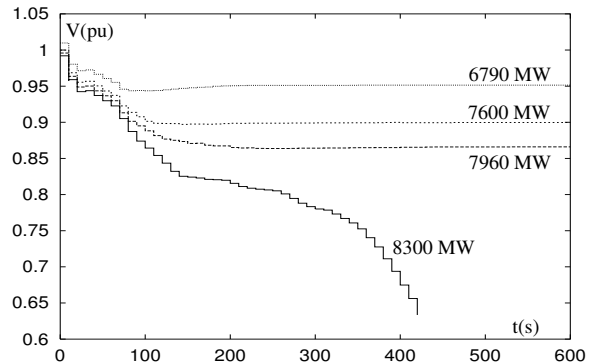


Fig. 9. Post-contingency voltage evolution at four pre-contingency load levels

Thus, if the load increase is larger than 8300 MW, the system response is unstable. To identify at which buses remedial actions should be taken, the $\partial V_\ell / \partial \mathbf{p}$ sensitivities are computed at the critical point of this unstable trajectory. This leads to the ranking of the 20 most effective reactive power injections shown with solid line in Fig. 10.

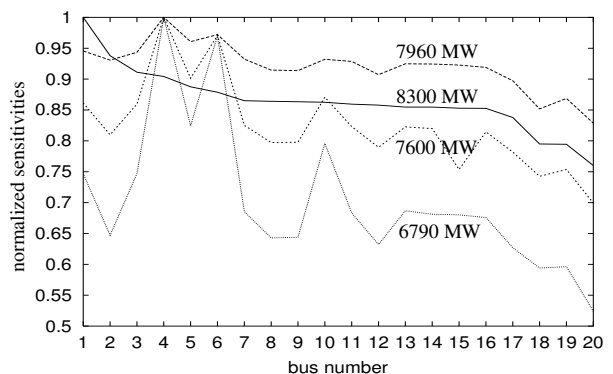


Fig. 10. Ranking of reactive power injections to stabilize or increase post-contingency voltages

If the load is increased by 7960 MW, the system is stable but the voltage settles down at 0.87 pu. If this value is deemed too low, the $\partial V_\ell / \partial \mathbf{p}$ sensitivities point out at which buses to act in order to raise this (stable but) low voltage. Note that in this case, no critical point is crossed along the trajectory and, hence, the sensitivities are computed at the final operating point. Their values are shown in Fig. 10 for the 20 reactive power injections best ranked in the unstable case.

Similarly, the figure shows the ranking determined at the final operating point when the load is increased by 7600 (respectively 6790) MW, which leads to a post-contingency voltage above 0.90 (respectively 0.95) pu.

The curves clearly show that the best buses to act on change when the requirement changes from stabilizing the system to obtaining higher and higher post-contingency voltages.

One can also observe that the smaller the pre-contingency load level, the larger the differences from one reactive power

injection to another.

IV. ON THE USE OF THE SENSITIVITIES

The standard practice is to operate power systems in a secure way with respect to credible (typically N-1 and some pre-defined N-2) contingencies and to deal with more severe (N-2 or higher) contingencies through emergency control (system protection schemes). Thus, N-1 contingencies are usually involved in preventive pre-contingency control while N-2 or higher contingencies are counteracted by emergency post-contingency controls.

As regards pre-contingency preventive control, the sensitivities can be used to reschedule generation (and in some cases, shed load) in order to make the system secure with respect to N-1 contingencies. One possibility is to use the sensitivities to rank the controls and then iteratively determine the total change in controls using nonlinear simulation [12]. Alternatively, linear inequality constraints can be derived from the sensitivities and embedded in an optimization formulation [13], [18].

As regards emergency post-contingency control, the sensitivities can be used to identify the most effective load shedding locations in an unacceptable post-contingency situation, as detailed in [12]. This information can be used in the design of an undervoltage load shedding scheme.

The above analyses are performed beforehand, i.e. before the contingency occurs, by simulating the impact of the contingency. As regards the possibility of computing the proposed sensitivities after the occurrence of a disturbance, the main obstacle lies in the fact that this computation involves a full network model. Today's SCADA systems cannot provide the dynamic evolution of the whole system state and wide area measurements cannot ensure full system observability. Now, as far as long-term voltage stability is of concern, an alternative would consist in identifying the disturbance and performing a faster than real-time QSS simulation to obtain the expected system evolution, starting from the pre-contingency state provided by the EMS state estimator.

V. CONCLUSION

This paper has revisited the use of sensitivities to identify which parameter changes are most effective to deal with unstable or low voltages. The emphasis is put on bus power injections, although other controls can be considered as well.

The proposed sensitivities focus on the weakest bus voltage, identified in practice as the one experiencing the largest drop due to the load increase or the contingency.

In voltage unstable cases, it has been shown that the proposed simple sensitivities, computed in the neighborhood of a saddle-node bifurcation or a critical point, yield essentially the same bus power ranking as the eigenvector computation proposed in previous works on the subject.

With respect to the latter, the sensitivity computation offers three advantages:

- *efficiency*: both approaches require a single computation and factorization of the Jacobian \mathbf{f}_x . However, the proposed sensitivities require to solve a single sparse linear

system, while the eigenvector computation requires to solve a sequence of such systems;

- *reliability*: eigenvector computation may experience convergence problems when the dominant eigenvalue does not go smoothly through zero but rather “jumps” from a negative to a (non negligible) positive value (e.g. around breaking points). On the other hand, the proposed sensitivities can always be computed which make them very reliable for practical applications;
- *extension to low but stable voltage problems* where eigenvector analysis does not apply in principle.

The sensitivities can be used in planning, operational planning (day ahead) and real time, complementing the existing analysis methods at a very little computational cost.

ACKNOWLEDGMENTS

We thank the RTE (France) and Hydro-Québec (Canada) companies for making realistic data available to us in order to perform this study.

REFERENCES

- [1] C.W. Taylor, *Power system voltage stability*, EPRI Power System Engineering Series, Mc Graw-Hill, 1994
- [2] P. Kundur, *Power System Stability and Control*, EPRI Power System Engineering Series, Mc Graw-Hill, 1994
- [3] T. Van Cutsem, C. Vournas, *Voltage Stability of Electric Power Systems*, Boston, Kluwer Academic Publishers, 1998
- [4] “Techniques for power system stability limit search”, IEEE PES special publication IEEE TP-138-0, Jan. 2000
- [5] “Voltage Stability Assessment: concepts, practices and tools”, Special publication of the IEEE Power System Stability Subcommittee (C. Cañizares, Editor), 2002, ISBN 0780378695
- [6] J. Peshon, D.S. Piercy, W.F. Tinney, O.J. Tveit, “Sensitivity in power systems”, IEEE Trans. on Power Apparatus and Systems, vol. PAS-87, 1968
- [7] “Indices predicting voltage collapse including dynamic phenomena”, Report of CIGRE Working Group 38.02.11, (J. Van Hecke, convenor), 1994
- [8] T. Van Cutsem, Y. Jacquemart, J.-N. Marquet, P. Pruvot, “A comprehensive analysis of mid-term voltage stability”, IEEE Trans. on Power Systems, Vol. 10, 1995, pp. 1173-1182
- [9] M. Begovic, A. Phadke, “Control of voltage stability using sensitivity analysis”, IEEE Trans. on Power Systems, Vol. 7, 1992, pp. 114-123
- [10] I. Dobson, “Observations on the geometry of saddle-node bifurcation and voltage collapse in electric power systems”, IEEE Trans. on Circuits and Systems-I, Vol. 39, No 3, 1992, pp. 240-243
- [11] S. Greene, I. Dobson, F. Alvarado, “Sensitivity of the loading margin to voltage collapse with respect to arbitrary parameters”, IEEE Trans. on Power Systems, Vol. 12, 1997, pp. 262-272
- [12] C. Moors, T. Van Cutsem, “Determination of optimal load shedding against voltage instability”, Proc. 13th Power System Computation Conference, Trondheim (Norway), July 1999, pp. 993-1000
- [13] F. Capitanescu, T. Van Cutsem, “Preventive control of voltage security: a multi-contingency sensitivity-based approach”, IEEE Trans. on Power Systems, Vol. 17, 2002, pp. 358-364
- [14] B. Gao, G.K. Morison, P. Kundur, “Voltage stability evaluation using modal analysis”, IEEE Trans. on Power Systems, Vol. 7, 1992, pp. 1529-1542
- [15] G.K. Morison, B. Gao, P. Kundur, “Voltage stability analysis using static and dynamic approaches”, IEEE Trans. on Power Systems, vol. 8, 1993, pp. 1159-1171
- [16] I. Dobson and L. Lu, “Immediate change in stability and voltage collapse when generator reactive power limits are encountered”, IEEE Trans. on Circuits and Systems I: Fundamental Theory and Applications, Vol. 39, No 9, 1992, pp. 762-766
- [17] N. Flatabo, R. Ognedal, T. Carlsen, “Voltage stability condition in a power system calculated by sensitivity methods”, IEEE Trans. on Power Systems, Vol. 5, No 4, 1990, pp. 1286-1293

- [18] F. Capitanescu, "Preventive assessment and enhancement of power system voltage stability: an integrated approach of voltage and thermal security", Ph.D. thesis, University of Liege, December 2003

Florin Capitanescu graduated in Electrical Power Engineering from the University "Politehnica" of Bucharest (Romania) in 1997. He received the D.E.A. and the Ph.D. degrees from the University of Liège in 2000 and 2003, respectively. His main current research interests are voltage stability and security analysis as well as applications of optimization methods.

Thierry Van Cutsem graduated in Electrical-Mechanical Engineering from the University of Liège in 1979, where he obtained the Ph.D. degree in 1984 and is now adjunct professor. Since 1980 he has been with the Belgian National Fund for Scientific Research (FNRS), of which he is now a Research Director. His research interests are in power system dynamics, stability, security and real-time control, in particular voltage stability and security.